FULL PAPER

Synthesis and Application of Na_2O/ZrO_2 Nanocomposite for Microwave-assisted Transesterification of Castor Oil

Dian Hidayat,[a] Akhmad Syoufian,[a] Hasanudin,[b] Maisari Utami,[c] Karna Wijaya [a,*]

Transesterification reaction of castor oil catalyzed by Na_2O/ZrO_2 to produce biodiesel has been investigated. The catalyst was made by activating the ZrO_2 with 98% NaOH 5 M, dried in oven for 24 hours, and followed by calcination in a muffle furnace at 500 °C for 5 hours. XRD analysis shows that the catalyst has typical peaks at $2\theta = 38.32°$, 33.19°, and 54.97°. The activation of the catalyst led to an increase of wt% of O and Na, but reduce the wt% of Zr. Transesterification of castor oil was carried out by varying the catalyst composition(w/w%) to determine its optimum conversion into product. The products were analyzed by GC-MS to determine the content and composition of the compounds, IR Spectroscopy to identify the functional group of the product, and ASTM analysis method to compare the quality of the product to the standard. The transesterification of castor oil was found to be optimum at 4% catalyst with biodiesel yield of 57.02%. However, the highest yield of methyl ester of ricinoleic acid, at 89.72%, was obtained using 2% catalyst (w/w%).

1 Introduction

Energy is always needed in human activities for continuing economic growth and living. Indonesia has an energy reserve, especially fossil fuels which are limited and non-renewable, whereas energy consumption in industries and transportation sectors are increasing. To avoid energy crisis, many efforts have been done to find alternative fuel that can fulfill the energy demand, while mitigating climate change. Many countries have started to reduce its dependence on fossil fuel by supporting the industry of biofuel[1,2], especially in the production of biodiesel. The attempts to produce biodiesel from biomasses such as palm oil, vegetables oil, and plant oil, have been widely reported[3]. Second generation of biodiesel is made from cooking oil, cotton seed oil and tobacco oil; including animal fats and used cooking oil[4]. Castor oil is considered to have a bright prospect as a biomass for biodiesel.

The conversion of biomass into biofuel can be significantly improved by introducing an effective catalyst with high activity and selectivity. Among the catalyst materials, zirconia has intrinsic advantages in stability and chemical resistance[5]. The synthesis of zirconium-based catalysts has been reported, such as $Cu–ZnO/Al_2O_3$ catalyst[6], $Cu/Ga_2O_3/ZrO_2$ and Cu/ZrO_2 catalysts[7]. However, the specific surface area of zirconia is typically smaller compared to other similar catalysts, like alumina or silica; thus increasing the specific surface area of zirconia particle has become a subject of interests. In this research, zirconia catalyst activated by sodium hydroxide (Na_2O/ZrO_2) was prepared and applied to the transesterification of castor oil.

2 Methodology

2.1 Materials and instrumentations

The materials used for this research were zirconia (obtained from BATAN), castor oil (PT. Brataco Chem), 98% NaOH, methanol, sulfate anhydrous (Merck/pro-analysis), distillate water. Instruments used were Fourier Transform Infra Red (FT-IR, Shimadzu-Prestige 21), Gas chromatography-Mass Spectrometer (GC-MS, Shimadzu QP-20105), X-ray Diffractometer (XRD, Shi-

[a] Physical Chemistry Laboratory, Chemistry Department, Faculty of Mathematics and Natural Science, Universitas Gadjah Mada, Sekip Utara, Yogyakarta 55281, Indonesia

[b] Physical Chemistry Laboratory, Chemistry Department, Faculty of Mathematics and Natural Science, Universitas Sriwijaya, Inderalaya, South Sumatera, Indonesia

[c] Chemistry Department, Faculty of Mathematics and Natural Sciences, Universitas Islam Indonesia, Yogyakarta 55584, Indonesia

[*] Corresponding author: karnawijaya@ugm.ac.id

madzu 6000), Scanning Electron Microscope Energy Dispersive X-Ray (SEM-EDX, located in Universitas Negeri Malang), H-NMR spectroscopy (located in LIPI), ASTM analyser (Chemical Engineering, located in Universitas Gadjah Mada).

2.2 Catalyst preparation and characterization

The activation of zirconia was initiated by dissolving the zirconia into NaOH 5 M. The ratio (w/w%) between zirconia and sodium hydroxide was 1:15. As much as 10 g of zirconia was dissolved in 150 mL of NaOH solution. The mixture of NaOH and zirconia was stirred for 24 hours, and then dried in an oven at 110 °C for 24 hours. The activated zirconia was calcined in a muffle furnace at 500 °C for 5 hours. The catalyst was characterized using FT-IR, XRD, and SEM-EDX. The crystallinity of zirconia was compared using the characteristic peaks obtained from Na_2CO_3 JCPDS card.

2.3 Transesterification of castor oil

Transesterification of castor oil to biodiesel was carried out by mixing castor oil with methanol at a ratio of 1:12. Activated zirconia catalyst was added at varied amounts of 1%, 2%, 3%, 4% of the oil weight. The mixtures were refluxed together in a 500 mL five-neck reaction flask, equipped with a condenser and stirrer, in a microwave at 700 W for 10 min. The liquid phase containing biodiesel and methanol was then separated from the solid catalyst by centrifugation at 2000 rpm for 10 min. The decanted liquid phase was then transferred to a rotary vacuum evaporator to remove the methanol from the biodiesel, followed by the addition of anhydrous Na_2SO_4 to absorb any excess water from the biodiesel[8].

3 Results and discussion

3.1 Crystallinity analysis using XRD

Figure 1 shows the XRD patterns from ZrO_2 and Na_2O/ZrO_2 nanocomposite. The XRD pattern of pure ZrO_2 exhibit typical diffraction peaks at $2\theta = 27.8°$, $31.25°$, and $49.50°$. According to JCPDS card with reference code 00-002-0536, it has been known that pure ZrO_2 is a monoclinic crystal system, while Na_2O/ZrO_2 nanocomposite shows peaks assigned to both the tetragonal and the monoclinic phases of zirconia. On Na_2O/ZrO_2 nanocomposite, the typical Na_2O peaks were observed at the Bragg angles, $2\theta = 38.32°$, $33.19°$, and $54.97°$. The phase change occurred when ZrO_2 is impregnated on a metal oxide, and its crystal structure will be changed from monoclinic to tetragonal[9]. An additional Na_2O/ZrO_2 phase appeared clearly in the diffraction patterns of the catalyst. The peak associated with Na_2O/ZrO_2 phase is observed at $2\theta = 15.81°$ as a result of the incorporation of Na^+ ions into the vacant site of zirconia with hydroxyl groups to form Na-O-Zr on the surface during calcination[8]. From the diffraction patterns above, there was no peak of $NaOH \cdot H_2O$ and there was a peak of $Na_2O_2 \cdot 8H_2O$. Arzamendi[10] reported that peaks with low intensity around $2\theta = 25°$, $27°$, $30°$, $27°$ were formed in the case of $NaOH \cdot H_2O$ and $Na_2O_2 \cdot 8H_2O$. The peak at $2\theta = 32.32°$ could be as a result of the incorporation of Na_2CO_3. This phenomena indicates that Na_2O/ZrO_2 nanocomposite has a tendency to absorb CO_2 from the environment[11].
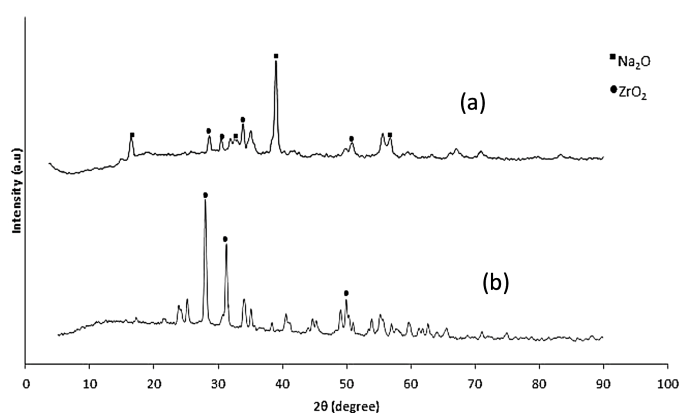

Figure 1 X-ray diffraction patterns of (a) pure ZrO_2, and (b) Na_2O/ZrO_2
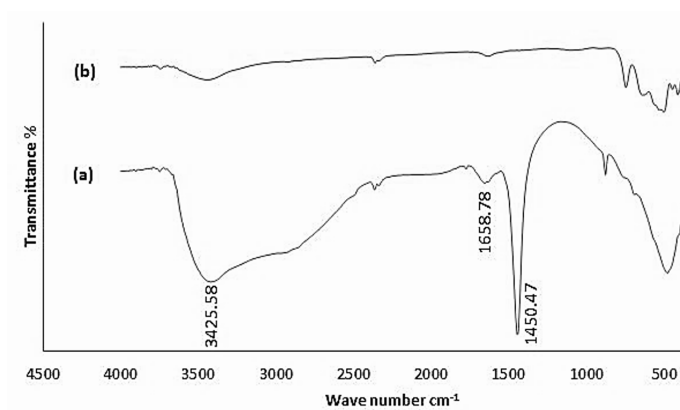

Figure 2 FT-IR spectra of (a) Na_2O/ZrO_2, and (b) pure ZrO_2

3.2 Functional group analysis using FT-IR

Qualitative analysis has been done by using FT-IR to identify functional group of the catalyst. FT-IR spectra of ZrO_2 and Na_2O/ZrO_2 nanocomposite catalysts were also examined and are shown in Figure 2. The spectra of Na_2O/ZrO_2 nanocomposite indicates a sharp peak at $1450.47\,cm^{-1}$ could be partly assigned to the vibration of carbonate ion (CO_3^{2-}) on the surface of Na_2O/ZrO_2 nanocomposite, which indicates that Na_2O/ZrO_2 nanocomposite has a tendency to absorb CO_2 from the environment[11]. Blunt peaks at $1658.78\,cm^{-1}$ and $3425.58\,cm^{-1}$ could be attributed to bending and stretching vibration of water[8], respectively.

3.3 Na_2O/ZrO_2 nanocomposite catalyst characterization using SEM-EDX

Figure 3 shows the surface topology of ZrO_2 and Na_2O/ZrO_2. The crystallites particle of ZrO_2 and Na_2O/ZrO_2 nanocomposite samples were each $20\,\mu m$. Fresh crystalline morphologies were formed at the surface of the prepared catalyst. There was a reduction in the particle sizes of the catalyst as a result of loading NaOH. However, there was significant difference could be observed between ZrO_2 and Na_2O/ZrO_2 nanocomposite images, indicating a good dispersion of NaOH on the surface of ZrO_2[8]. Based on the percentage of NaOH mass loaded on ZrO_2, there has been a decline in mass percentage of Zirconia on Na_2O/ZrO_2 nanocomposite. The Na^+ ion of NaOH could have been inserted
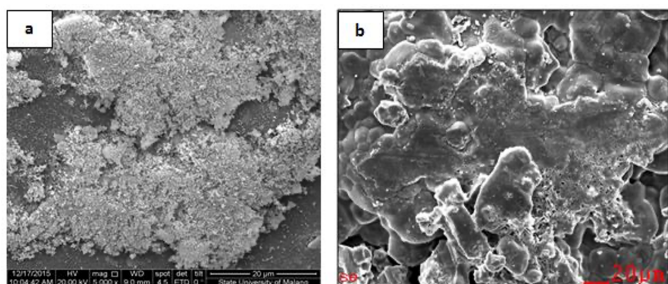
Figure 3 SEM image of (a) pure ZrO_2, and (b) Na_2O/ZrO_2

**Table 1** The amount of Atoms Oxygen (O), Sodium (Na) and Zirconia (Zr)

Atom	Pure ZrO_2 (wt%)	Na_2O/ZrO_2 (wt%)
O	20.72	34.08
Na	-	57.21
Zr	79.28	8.71

Figure 4 Effects of the amount of the Na_2O/ZrO_2 catalyst on the yield of biodiesel under a microwave system

Figure 5 Effects of the amount of the catalyst on the methyl ester of ricinoleic yield

in the vacant sites of ZrO_2 which accelerated dissociative dispersion and decomposition of NaOH to form basic sites in the activation process. It has been reported that the more KOH was loaded on ZrO_2, the more free vacant sites of ZrO_2 decreases[8]. Clearly, ZrO_2 retained its structure after NaOH loading, which is important for its catalytic activity. Sodium species could be found distributed on the surface of the support. The largest amounts of wt% were Na_2O/ZrO_2 nanocomposite while the smallest were ZrO_2. The difference amount (wt%) of Na, O and Zr were examined in Table 1. The amount (wt%) of Zr decreased from 79.28% to 8.71%, while the amount (wt%) of O increased from 20.72% to 34.08% after activated by NaOH. The activation was successfully done, as indicated by the percentage (wt%) of Na loaded on ZrO_2.

3.4 Transesterification of Castor Oil Catalyzed by Na_2O/ZrO_2 Nanocomposite Catalyst

In transesterification process, triglyceride is successively transformed into diglyceride, monoglyceride, and to glycerine and FAME[8]. The molar ratio of methanol to oil and reaction time affect the conversion of triglycerides to esters[12]. Microwave-assisted transesterification reaction is related to adsorption of microwave radiation by polar groups (OH) from the reagent[13]. Experiments were carried out using different amount of the catalysts, i.e. 1, 2, 3, 4, and 5 wt%, in order to investigate their influence on the product yield. The microwave system was operated at 700 W, with a reaction time of 10 min, and a methanol-to-oil molar ratio of 1:12.

Figure 4 shows the influence of the catalyst to transesterification process of castor oil to produce biodiesel. Conversion of biodiesel is expected to improve when the amount of catalyst is increased. Figure 4, shows that the yield tends to increase with the increasing amount of catalyst up to 4 wt%, while safonification reaction occured instead for catalyst concentration of 5 wt%. The highest yield was obtained with 4 wt% Na_2O/ZrO_2. Although
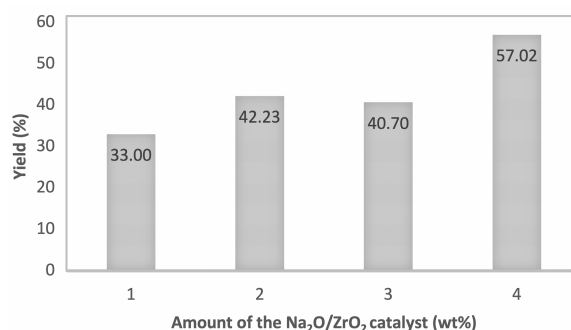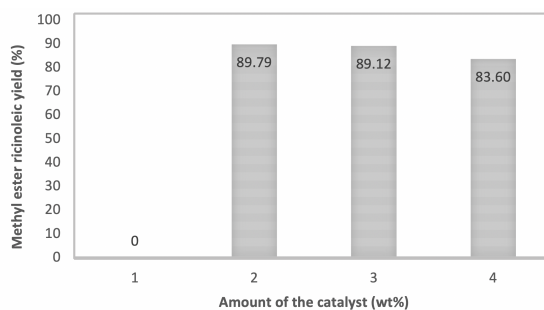
an excess catalyst might increase the biodiesel yield, the amount of glycerin produced is also increased due to saponification, causing a reduction of biodiesel yields. A further increase in catalyst concentration did not increase the conversion. Instead, it would led to extra costs due to the need to recover catalysts at the end of the conversion process[14].

3.5 Biodiesel characterization

The obtained biodiesel from castor oil was characterized using GCMS, FT-IR, and ^{1}H-NMR. The biodiesel is also characterized using ASTM method to understand its physical property.

3.5.1 GC-MS analysis

GC-MS analysis indicated the presence of methyl ester of ricinoleic acid which was produced from transesterification reaction using microwave catalysed by Na_2O/ZrO_2. The yields of methyl ester of ricinoleic as a function of catalyst amounts, as shown in Figure 5, were particularly high when the amount of catalyst involve was 2-4%. Figure 6 shows sample chromatogram of the biodiesel produced from transesterification using 2% catalyst. The chromatogram consists of seven peaks which indicate that there were at least seven compounds in the obtained biodiesel. Retention time, area percentage and the compounds that correspond to each peak are listed in Table 2. The seventh peak with area percentage of 89.73% and retention time of 49.551 min belong to methyl ester of ricinoleic acid. When compared to the standard of methyl ester of ricinoleic acid, it has a similarity indeks of 93%.
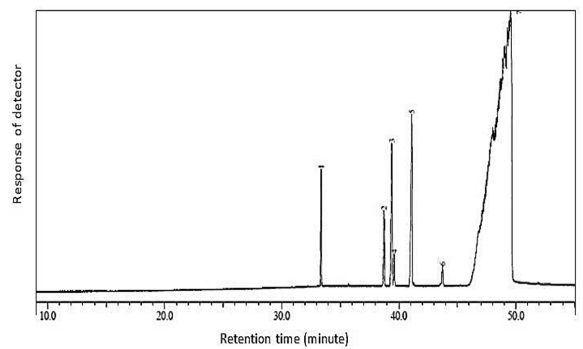
Figure 6 Chromatogram of biodiesel from castor oil

Table 2 Retention time t_{ret} and area percentage for seven peaks of GC chromatogram

Peaks	t_{ret} (min)	Area%	Compounds
1	33.372	1.17	hexadecanoic acid
2	38.735	1.37	methyl stearate
3	39.412	2.90	11-octadecenoic acid
4	39.610	0.52	12-octadecenoic acid
5	41.112	3.97	methyl linoleic
6	43.738	0.33	9,12,15-octadecatrienoic
7	49.551	89.73	methyl ester of ricinoleic acid

3.5.2 ^{1}H-NMR spectrometer analysis

Analysis using ^{1}H-NMR was done to clarify the purity of biodiesel obtained from transesterification reaction of castor oil with methanol. Important peaks include the chemical shift of the peak at 4.1-4.4 ppm, which is proton-proton spectra of glyceride, and at 3.7-4.0 ppm, which is the proton spectra of methoxy group[15]. Figure 7 shows the peaks of triglyceride with a chemical shift at 4.1-4.3 ppm, integration value of 0.713 and 0.787. This triglyceride would be converted into methyl ester of ricionelic acid with transesterification reaction.

The ^{1}H-NMR spectrum of castor oil shows glyceride protons at 4.1-4.3 ppm, while the ^{1}H-NMR spectrum of biodiesel shows a strong singlet at 3.7 ppm with integration value of 3 that indicates the formation of methyl ester. The signals at 2.2 and 2.3 ppm result from the protons on the CH$_2$ groups adjacent to the methyl ester are shown in Figure 8. The disappearance of the glyceride protons at 4.1-4.3 ppm and the appearance of methyl ester protons at 3.6-3.7 ppm are two facts that differentiate castor oil from the resulting fatty acid methyl ester.

Number of conversion which has been obtained in this research of 67.92%. This value obtained from Knothe equation. Based on the obtained yield could be concluded that the conversion of castor oil become biodiesel has not maximum yet. This phenomena could be caused by some factors, such as concentration of the catalyst and time which is needed in transesterification reaction with microwave system produce methyl ester.

3.5.3 Infrared (FT-IR) spectrometer analysis

Ricinoleic acid is the major component in castor oil, which contains a hydroxyl component, presenting bands at 3440, 850, and 1000 cm^{-1}. In the FT-IR analysis of biodiesel, the intense C=O stretching band of methyl ester was presented at 1742 cm^{-1} and medium C-O bands were presented at 1173, 1200, and 1246 cm^{-1} [16]. The characteristic peaks of biodiesel and castor oil were similar, and no significant difference could be observed between biodiesel and castor oil in the Figure 9.

3.6 Biodiesel properties to national standard

Analysis of biodiesel properties was conducted and the results were compared to national standards of Indonesia through several parameters such as density, viscosity kinematic, flash point, and pour point. Table 3 shows comparison of castor oil biodiesel properties to national standards SNI-04-7182-2006. Based on the Table 3, it can be shown that the process of transesterification reaction with heterogenous catalyst Na$_2$O/ZrO$_2$ has changed the physical properties of castor oil into biodiesel as a fuel source. Specific density at temperature 15 °C measured with ASTM method D 1298 was 0.9469 g cm^{-3} based on SNI-04-7182-2006. This value indicates that the biodiesel produced has density higher than standard. The density of biodiesel is typically higher than that of diesel fuel and is dependent on fatty acid composition and purity[17].

Kinematic viscosity is one of the test parameters that express the resistance of a fuel to flow. Viscosity values will affect the lubrication fuel injectors, biodiesel with high viscosity fuel causes difficult sprayed or atomized. Kinematic viscosity test value of biodiesel castor oil was 77.03 mm^2 s^{-1}. This value is larger than a standard diesel oil according to SNI-04-7182-2006, but viscosity of biodiesel can be lowered by the addition of a diluent such as ethyl astetoacatate because it has smaller viscosity (1.63 mm^2 s^{-1}; 40 °C) compared to biodiesel[18]. It also can be caused by the mixing of KOH with methanol that produced a small amount of water. The water then facilicated the hydrolisis of ester that led in soap formation[14].

Flash point is the lowest temperature at which a fuel can be ignited. If a fuel has a flash point that is lower than standard (100 °C), the fuel would be considered dangerous for storage. The flash point of biodiesel from castor oil was at 111 °C, the value appropriated to standard SNI-04-7182-2006 as a fuel. Flash point of biodiesel products in this study indicates that the residual methanol reaction was slight, because methanol in considerable amounts in biodiesel will lower the flash point.

Pour point indicates the lowest temperature at which fuel can be streamed or poured out. High pour point makes an engine difficult to be initiated at low temperatures[19]. The pour point of biodiesel from castor oil was shown to be 27 °C. This indicates that the biodiesel from castor oil is suitable for both tropical and sub-tropical countries.

4 Conclusions

Activation of the zirconia catalyst increased the percentage of O, Na, but reduce the percentage of Zr. The transesterification reaction of castor oil using 4% w/w activated Na$_2$O/ZrO$_2$ nanocomposite catalyst gave biodiesel with yield of 57.02%. The highest yield of methyl ester of ricinoleic acid, at 89.79%,
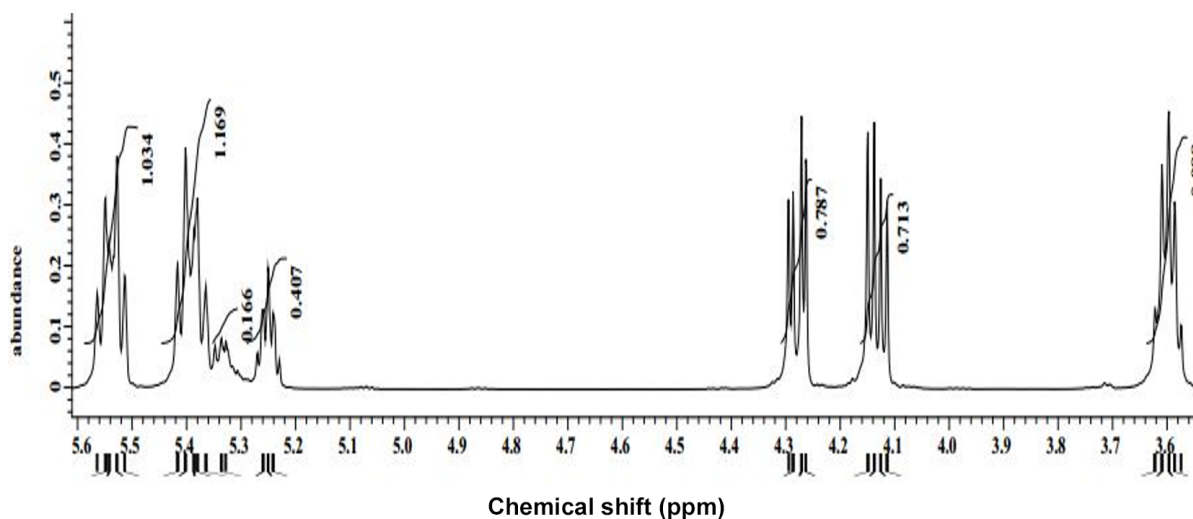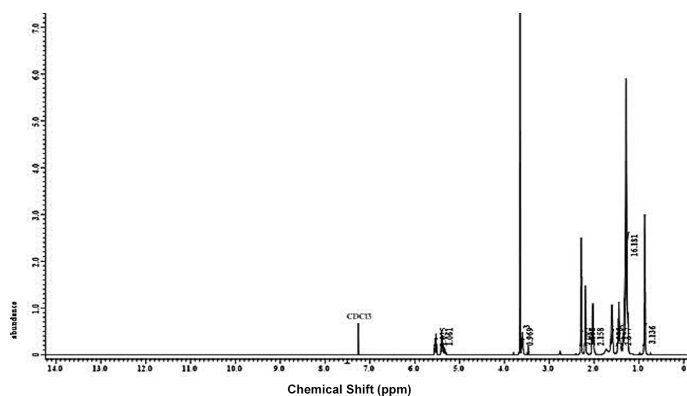
Figure 7 ^{1}H-NMR spectra of castor oil

Figure 8 ^{1}H-NMR spectra of biodiesel from castor oil
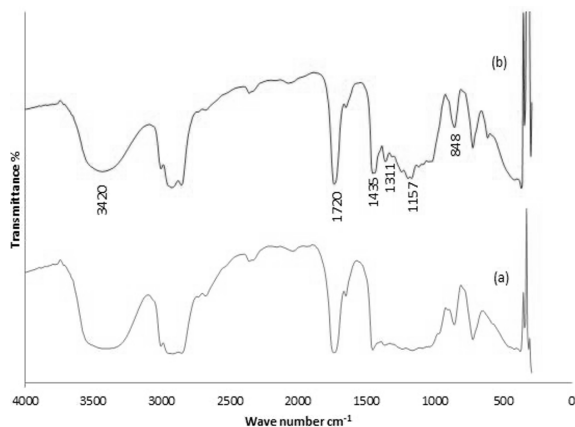

Figure 9 FT-IR spectra of (a) castor oil and (b) biodiesel

Table 3 Comparison of castor oil to Indonesia National Standards (SNI-04-7182-2006)

Parameter	Unit	Diesel[*]	Castor oil biodiesel
Density at 15 °C	$g\,cm^{-3}$	0.85 - 0.92	0.9469
Viscosity Kinematics at 40 °C	$mm^2\,s^{-1}$	2.3 - 6.0	77.03
Flash Point	°C	Min. 100	111.0
Pour point	°C	Max. 18	-18

[*] SNI-04-7182-2006 issued by National Standardization Agency of Indonesia.

was obtained with 2% w/w amounts of catalyst. The chromatogram of GC-MS showed that the obtained biodiesel consisted of hexadecanoic acid, methyl stearate, 11-octadecenoic acid, 12-octadecenoic acid, methyl linoleic, 9,12,15-octadecetrienoic and methyl ester of ricinoleic acid. The biodiesel produced from castor oil has a flash point and a pour point that met the standard of biodiesel. However, the density and viscosity kinematic of this biodiesel did not meet the standard of biodiesel yet.

Acknowledgements

References

1 N. Idusuyi, O. Ajide and R. Abu, Biodiesel as an Alternative Energy Resource in Southwest Nigeria, *International Journal of Science and Technology*, 2012, **2**, 323–327.

2 K. Chen, L. Zhang, M. Gholizadeh, N. Ai, M. M. Hasan, D. Mourant, C.-Z. Li and S. P. Jiang, Feasibility of tubular solid oxide fuel cells directly running on liquid biofuels, *Chemical Engineering Science*, 2016, **154**, 108–118.

3 G. Kafuku and M. Mbarawa, Biodiesel production from *Croton megalocarpus* oil and its process optimization, *Fuel*, 2010, **89**, 2556–2560.

4 A. S. Silitonga, A. E. Atabani, T. M. I. Mahlia, H. H. Masjuki,

I. A. Badruddin and S. Mekhilef, A review on prospect of *Jatropha curcas* for biodiesel in Indonesia, *Renewable and Sustainable Energy Reviews*, 2011, **15**, 3733–3756.

5 M. Fan, Z. Si, W. Sun and P. Zhang, Sulfonated ZrO_2-TiO_2 nanorods as efficient solid acid catalysts for heterogeneous esterification of palmitic acid, *Fuel*, 2019, **252**, 254–261.

6 Y. Zhuang, R. Currie, K. B. McAuley and D. S. A. Simakov, Highly-selective CO_2 conversion via reverse water gas shift reaction over the 0.5wt% Ru-promoted $Cu/ZnO/Al_2O_3$ catalyst, *Applied Catalysis A: General*, 2019, **575**, 74–86.

7 E. L. Fornero, D. L. Chiavassa, A. L. Bonivardi and M. A. Baltanás, Transient analysis of the reverse water gas shift reaction on Cu/ZrO_2 and $Ga_2O_3/Cu/ZrO_2$ catalysts, *Journal of CO_2 Utilization*, 2017, **22**, 289–298.

8 M. Takase, M. Zhang, W. Feng, Y. Chen, T. Zhao, S. J. Cobbina, L. Yang and X. Wu, Application of zirconia modified with KOH as heterogeneous solid base catalyst to new non-edible oil for biodiesel, *Energy Conversion and Management*, 2014, **80**, 117–125.

9 Y. Li, B. Ye, J. Shen, Z. Tian, L. Wang, L. Zhu, T. Ma, D. Yang and F. Qiu, Optimization of biodiesel production process from soybean oil using the sodium potassium tartrate doped zirconia catalyst under Microwave Chemical Reactor, *Bioresource Technology*, 2013, **137**, 220–225.

10 G. Arzamendi, I. Campo, E. Arguiñarena, M. Sánchez, M. Montes and L. Gandía, Synthesis of biodiesel with heterogeneous NaOH/alumina catalysts: Comparison with homogeneous NaOH, *Chemical Engineering Journal*, 2007, **134**, 123–130.

11 A. S. Silitonga, A. H. Shamsuddin, T. M. I. Mahlia, J. Milano, F. Kusumo, J. Siswantoro, S. Dharma, A. H. Sebayang, H. H. Masjuki and H. C. Ong, Biodiesel synthesis from Ceiba pentandra oil by microwave irradiation-assisted transesterification: ELM modeling and optimization, *Renewable Energy*, 2020, **146**, 1278–1291.

12 W. K. Teng, G. C. Ngoh, R. Yusoff and M. K. Aroua, Microwave-assisted transesterification of industrial grade crude glycerol for the production of glycerol carbonate, *Chemical Engineering Journal*, 2016, **284**, 469–477.

13 K.-S. Chen, Y.-C. Lin, K.-H. Hsu and H.-K. Wang, Improving biodiesel yields from waste cooking oil by using sodium methoxide and a microwave heating system, *Energy*, 2012, **38**, 151–156.

14 M. W. Majewski, S. A. Pollack and V. A. Curtis-Palmer, Diphenylammonium salt catalysts for microwave assisted triglyceride transesterification of corn and soybean oil for biodiesel production, *Tetrahedron Letters*, 2009, **50**, 5175–5177.

15 P. D. Rocha, L. S. Oliveira and A. S. Franca, Sulfonated activated carbon from corn cobs as heterogeneous catalysts for biodiesel production using microwave-assisted transesterification, *Renewable Energy*, 2019, **143**, 1710–1716.

16 Gisela Montero and Margarita Stoytcheva, *Biodiesel - Quality, Emissions and By-Products.*, Technical University of Cluj-Napoca, Romania, 2011.

17 L. Cao, J. Wang, K. Liu and S. Han, Ethyl acetoacetate: A potential bio-based diluent for improving the cold flow properties of biodiesel from waste cooking oil, *Applied Energy*, 2014, **114**, 18–21.

18 Sukmana, Ndaru Candra and Purwanti, Endang, Kalor Biodiesel Hasil Esterifikasi dengan Katalis Asam Sitrat dan Transesterifikasi dengan Katalis Kalium Hidroksida Minyak Biji Nyamplung (*Calophyllum inophyllum*), Prosiding Tugas Akhir, Surabaya, 2011, 1–11.

19 V. L. Maleev, *Diesel engine operation and maintenance: the construction, operation, maintenance, and repair of modern diesel engines*, McGraw-Hill, New York, 1954.